

1 Ammonia and nitrite oxidation in the upper euphotic zone of the oligotrophic Red Sea

2 Eyal Rahav^{1,2,3*}, Scott D Wankel⁴, and Adina Paytan²

3
4 ¹ Israel Oceanographic and Limnological Research, Haifa, Israel.

5 ² Institute of Marine Science, University of California, Santa Cruz, CA, USA.

6 ³ Department of Earth and Environmental Science, Ben-Gurion University of the Negev, Beer
7 Sheva, Israel.

8 ⁴ Marine Chemistry and Geochemistry Department, Woods Hole Oceanographic Institution,
9 Woods Hole, Massachusetts, USA.

10
11 *Corresponding author: eyrahav@ucsc.edu; eyal.rahav@ocean.org.il

12 13 **Abstract**

14 Nitrification is widely understood to be inhibited by light in the surface ocean, however,
15 increasing evidence indicates its occurrence at low levels at many sites. The extent to which
16 nitrification remains active in the euphotic zone could have important implications to new
17 production calculations, yet it remains understudied. Here, we quantified ammonia and nitrite
18 oxidation rates in the euphotic zone of the Gulf of Aqaba (Northern Red Sea) from late spring
19 to late summer and examined environmental controls and implications for dark carbon fixation
20 (chemoautotrophy) and new production. Both ammonia and nitrite oxidation were detectable
21 throughout the euphotic zone ($\sim 0.1\text{-}0.8 \text{ nmol N L}^{-1} \text{ d}^{-1}$). Overall, rates were low in the highest-
22 irradiance surface waters and increased with depth. Integrated rates over the entire euphotic
23 zone ($24\text{-}56 \text{ }\mu\text{mol N m}^{-2} \text{ d}^{-1}$) were among the lowest reported for oligotrophic regions globally.
24 This reflects extremely low substrate concentrations and intense, though not complete, photo-
25 inhibition. Ammonia and nitrite oxidation together supported $<2\%$ of dark carbon fixation
26 rates, suggesting other processes, not accounted for, drive this chemoautotrophic activity.
27 Depth-resolved correlations with environmental parameters highlight light, temperature, and
28 substrate availability as key regulators of both processes. Our results show that nitrification in
29 the Gulf of Aqaba operates at the lower bounds of global euphotic zone rates and is loosely
30 coupled to carbon cycling. These findings underscore the need to better resolve nitrification
31 dynamics in ultra-oligotrophic, rapidly warming, seas to refine estimates of new production
32 and chemoautotrophic carbon assimilation under future ocean conditions.

33

34 **Key words:** Ammonia oxidation, Nitrite oxidation, Dark carbon fixation, Red Sea,
35 Oligotrophic.

36

37 **1 Introduction**

38 Nitrification, the sequential oxidation of ~~ammonium ammonia~~ (NH_4^+) to nitrite (NO_2^-)
39 followed by the oxidation of nitrite to nitrate (NO_3^-), is a microbially mediated process central
40 to the regulation of nitrogen availability across nearly all aquatic environments, linking the
41 most reduced and oxidized states of nitrogen (Ward, 2008). Although nitrification does not
42 change the absolute inventory of bioavailable nitrogen (N) in the oceans, it alters the balance
43 among nitrogen species that serve as substrates for different organisms, thereby affecting
44 phytoplankton species abundance and growth (Fawcett et al., 2011). Ammonia oxidation is
45 carried out by ammonia-oxidizing archaea and bacteria (Francis et al., 2005; Wuchter et al.,
46 2006), while nitrite oxidation is performed by nitrite-oxidizing bacteria (Mincer et al., 2007;
47 Pachiadaki et al., 2017). Ammonia-oxidizing bacteria that perform the entire process have also
48 been identified in freshwater, terrestrial, and coastal habitats, but have not yet been found in
49 the open ocean (Daims et al., 2015; Fei et al., 2018; van Kessel et al., 2015).

50 Nitrification has been investigated across a wide range of marine settings, including the
51 Atlantic (Clark et al., 2008, 2022), the Pacific (Wan et al., 2021; Wankel et al., 2007), and the
52 Polar (Mdutyana et al., 2020; Shiozaki et al., 2019) ocean basins, as well as numerous coastal
53 and estuarine systems (Henriksen and Kemp, 1988; Herbert, 1999; Zhu et al., 2018). As a
54 chemoautotrophic process, nitrification contributes to organic carbon production in the ocean
55 interior (Middelburg, 2011; Pachiadaki et al., 2017), and may fuel bacterial carbon demand and
56 support heterotrophic food-webs in the mesopelagic and bathypelagic water depths (Bayer et
57 al., 2025). The activity of nitrifiers is known to be promoted or inhibited by many
58 environmental factors (Ward, 2008), yet specific controls on its occurrence in the water column
59 and broader ecological implications across different ocean settings remain poorly constrained
60 (Tang et al., 2023). Additionally, because uptake of NH_4^+ and NO_3^- has long served to
61 differentiate between ‘regenerated’ and ‘new’ production, respectively (Eppley and Peterson,
62 1979), *in situ* production of NO_3^- by nitrification in the photic zone skews global estimates of
63 new production and carbon export in the oceans (Yool et al., 2007; Wankel et al., 2007).

64 Here, we report ammonia and nitrite oxidation rates in the upper euphotic zone (surface
65 and down to ~100 m, representing 100% to ~0.5-1.8% of surface irradiance, respectively) of

66 the Gulf of Aqaba (GoA, Northern Red Sea) during late spring and throughout the summer
67 season. Rates were compared with common environmental physiochemical and biological
68 parameters to assess drivers of nitrification in this marine setting. Using these data, we provide
69 estimates of the contribution of ammonia and nitrite oxidation to dark carbon fixation (DCF)
70 and new production in ~~the~~ the oligotrophic, warm and well-lit GoA.

71 **2 Material and methods**

72 Seawater was collected every 20 m throughout the euphotic zone (0-100 m depth) at an
73 offshore, routinely monitored, station in the GoA ("Station A", latitude 29.47 N, longitude
74 34.92 E). Ammonia and nitrite oxidation rates were assessed using stable ^{15}N isotope
75 enrichment incubations. Five monthly sampling events were performed spanning late
76 spring/early summer (May) to late summer (September) in 2023, covering the period in which
77 the GoA is characterized by oligotrophic N-poor conditions (Fuller et al., 2005; Mackey et al.,
78 2007). Ancillary water column measurements included temperature, salinity, photosynthetic
79 active radiation (PAR) (Seabird 19 Plus), inorganic nitrogen species concentrations (NO_2^- ,
80 NO_3^- , NH_4^+), chlorophyll-*a*, and rates of photosynthesis and DCF.

81 **2.1 Inorganic nitrogen species**

82 Duplicate water samples for nitrite (NO_2^-) and nitrate (NO_3^-) were collected in 15 ml
83 acid-clean polyethylene tubes directly from Niskin bottles. Prior to filling, the tube was
84 thoroughly rinsed three times with sample water. After collection, samples were stored at 4 °C
85 in the dark and analyzed the following day. Nitrite (~~NO_2^-~~) and nitrate (~~NO_3^-~~) concentrations
86 were determined colorimetrically following standard procedures (Grasshoff et al., 1999).
87 Nitrite was measured directly using the Griess reaction, in which nitrite forms an azo dye after
88 reaction with sulfanilamide and N-(1-naphthyl)ethylenediamine and is quantified
89 spectrophotometrically ($\lambda=520$ nm). Nitrate was reduced to nitrite using a copper-coated
90 cadmium reduction column and subsequently $\text{NO}_2^- + \text{NO}_3^-$ was analyzed by the same azo-dye
91 method. Nitrate concentrations were then calculated by difference. Analyses were performed
92 using a Flow Injection Autoanalyzer system (FIA, Lachat Instruments Model QuikChem
93 8000). The analysis was automated, and peak areas were calibrated using standards prepared
94 in nutrient-deplete 0.2- μm filtered surface seawater from the GoA over a range of 0-100 nmol
95 L^{-1} . The detection limits were 10 nmol L^{-1} and 20 nmol L^{-1} for nitrite and nitrate, respectively,
96 with typical analytical precision of ~ 20 nmol L^{-1} , consistent with previous measurements in the
97 GoA (e.g., Mackey et al., 2011).

98 Samples for ammonia (NH_4^+) concentration were collected directly from Niskin bottles
99 into acid-washed plastic vials after rinsing 3 times with sample water. The collected samples
100 were stored in 4 °C in the dark and analyzed within an hour after collection. Ammonia
101 concentrations were determined using the orthophthaldialdehyde (OPA) method (Holmes et al.,
102 1999), where samples were first incubated with a working reagent of OPA for 3 h and then
103 measured fluorometrically (Turner Designs, Ex: 360 nm, Em. 420 nm). The detection limit ~~of~~
104 ~~the OPA analysis~~ was $\sim 4 \text{ nmol L}^{-1}$ (Meeder et al., 2012). Procedural blanks were routinely
105 measured and subtracted from sample signals to account for background contamination. Note
106 that calibration and quality control procedures were carried out during nutrient measurements.
107 The analytical precision and detection limits were within the expected range for oligotrophic
108 seawater measurements.

109 2.2 Ammonia and nitrite oxidation rates

110 Ammonia and nitrite oxidation rates were determined using stable isotope tracer
111 incubations (Beman et al., 2011; Bristow et al., 2015; Ward, 1987). Seawater was collected into
112 triplicate 1-L acid-cleaned transparent Nalgene bottles without headspace. The bottles were
113 incubated on land for 24 h in aquarium tanks continuously supplied with running surface
114 seawater, using neutral density screening nets simulating the light conditions of the collection
115 depth (no change in spectra). For ammonia oxidation, samples were amended with ^{15}N -labeled
116 ammonium chloride ($^{15}\text{NH}_4\text{Cl}$, $>98 \text{ atom } \%$; Cambridge Isotope Laboratories) at a
117 concentration of $\sim 20 \text{ nmol L}^{-1}$ which is sufficient to yield a quantifiable signal while potentially
118 introducing some degree of tracer perturbation (discussed below). For nitrite oxidation,
119 samples were amended with $\sim 5 \text{ nmol L}^{-1}$ of ^{15}N -labeled sodium nitrite ($^{15}\text{NO}_2^-$, $>98 \text{ atom } \%$),
120 thus minimally perturbing the *in situ* nitrite pool. At the end of the incubation, subsamples were
121 filtered onto a Supor 0.22 μm (47 mm) filter using gentle filtration, and the filtrate ($<0.22 \mu\text{m}$)
122 was kept frozen in the dark at $-20 \text{ }^\circ\text{C}$ until analysis. For ammonia oxidation, the presence of
123 $^{15}\text{NO}_2^-$ in the total dissolved nitrite pool was quantified by isotope ratio mass spectrometry
124 (IRMS).

125 For nitrite oxidation, we quantified the $^{15}\text{NO}_3^-$ in the dissolved nitrate pool after
126 conversion to nitrous oxide with subsequent IRMS analysis. The azide method (McIlvin and
127 Altabet, 2005) and the denitrifier method (Casciotti et al., 2002; Sigman et al., 2001), with
128 technical updates for low-concentration analysis (McIlvin and Casciotti, 2011), are well
129 established for isotopic analysis of nitrite and nitrate in oligotrophic seawater. Prior to
130 denitrifier analysis, nitrite was removed from nitrate samples using the sulfamic acid procedure

131 (Granger and Sigman, 2009) to ensure that the ^{15}N signal reflected only the nitrate
132 pool. Aliquots of 2-10 ml were introduced per denitrifier vial depending on ambient NO_3^-
133 concentration, consistent with the volume constraints of Sigman et al., (2001) and McIlvin and
134 Casciotti, (2011). For surface samples with the lowest NO_3^- concentrations sequential injections
135 of multiple aliquots from the same filtrate were used to accumulate sufficient N mass per vial,
136 while for deeper samples with higher NO_3^- single injections of 2-5 ml were sufficient. Given
137 that ambient NO_3^- and NO_2^- concentrations in GoA surface waters approached, or were below,
138 the validated concentration ranges of these methods, the analyses were performed with careful
139 attention to blank correction. Accordingly, rates derived from near-surface, low-concentration
140 samples were interpreted conservatively. For sequential-injection analyses of low-
141 concentration surface samples, the cumulative bacterial blank was estimated based on injection
142 number and subtracted accordingly; samples where the ^{15}N signal could not be distinguished
143 from the cumulative blank were excluded and treated as below the detection limit. In the most
144 oligotrophic surface samples these established approaches were applied near their practical
145 detection limits, and ^{15}N enrichments should therefore be regarded as conservative minimum
146 estimates rather than evidence that the bacterial and azide methods are routinely robust at
147 concentrations of only a few tens of nmol L^{-1} .

148 ~~For nitrite oxidation, we quantified the $^{15}\text{NO}_3^-$ in the dissolved nitrate pool after~~
149 ~~conversion to nitrous oxide via the denitrifier method (Sigman et al., 2001) and subsequent~~
150 ~~IRMS analysis. Note that in order to ensure sufficient nitrogen mass for isotopic analysis under~~
151 ~~low ambient nutrient concentrations, relatively large incubation volumes (1 L) were used, and~~
152 ~~a substantial fraction of the filtrate was processed for isotope measurements. The azide and~~
153 ~~denitrifier methods employed here are well established for the analysis of low concentration~~
154 ~~nitrite and nitrate pools and allow reliable detection of ^{15}N enrichment in oligotrophic systems~~
155 ~~. Recent methodological modifications involving anion-exchange resin enrichment coupled~~
156 ~~with azide reduction for low concentration nitrite isotope analysis were suggested to enhanced~~
157 ~~analytical sensitivity (Jiang et al., 2026); however, the established approaches used here are~~
158 ~~widely applied in oligotrophic systems and were sufficient for robust detection of ^{15}N~~
159 ~~enrichment in the present study.~~

160 Killed controls poisoned with HgCl_2 from each collection depth were incubated in
161 parallel to the experimental bottles to account for any abiotic transformations and subtracted
162 from the 'live' bottles. Rates in the 'mercury-killed' controls were typically negligible relative
163 to the 'live' bottles (usually $<0.05 \text{ nmol N L}^{-1} \text{ d}^{-1}$). The resulting detection limit, which was
164 defined as the mean killed-control rate plus three standard deviations, corresponded to 0.1 nmol

165 N L⁻¹ d⁻¹. Rates below this threshold were considered indistinguishable from background signal
166 and were interpreted as ‘below detection’. This operational detection limit is based on the
167 variability of killed controls and background signals and does not represent a full validation of
168 isotope analysis at ambient nitrite or nitrate concentrations of only a few tens of nmol L⁻¹.

169 Rates of ammonia and nitrite oxidation were calculated following previous studies (Beman et
170 al., 2011; Bristow et al., 2015; Ward, 1987) as shown in Equations 1-3:

171

172 (1) Ammonia oxidation =
$$\frac{\Delta (\text{atm}\% \text{ } ^{15}\text{N NO}_2) \times [\text{NO}_2]_{\text{final}}}{t \times F (\text{NH}_4)}$$

173

174 (2) Nitrite oxidation =
$$\frac{\Delta (\text{atm}\% \text{ } ^{15}\text{N NO}_3) \times [\text{NO}_3]_{\text{final}}}{t \times F (\text{NO}_2)}$$

175

176 (3) F substrate =
$$\frac{[^{15}\text{N substrate}]_{\text{added}}}{[\text{Substrate ambient}] + [\text{Substrate added}]}$$

177

178 Where, $\Delta(\text{atm}\% \text{ } ^{15}\text{N NO}_2^-)$ or $\Delta(\text{atm}\% \text{ } ^{15}\text{N NO}_3^-)$ = atom% excess ¹⁵N in the nitrite or nitrate
179 pool relative to natural abundance; $[\text{NO}_2^-]_{\text{final}}$ or $[\text{NO}_3^-]_{\text{final}}$ = final concentration of the nitrite
180 or nitrate pool (nmol L⁻¹); t = time (d); F_{NH4} or F_{NO2} = fractional ¹⁵N enrichment of the ammonia
181 or nitrite substrate pool.

182

183 Note that for the ammonia oxidation rates we added tracer additions which correspond
184 to 30-50% of the ambient NH₄⁺ concentrations. While we aimed to minimize substrate
185 perturbation, such additions are inherently challenging in ultra-oligotrophic systems, where
186 even low absolute tracer concentrations can represent a substantial fraction of the ambient pool
187 (Zheng et al., 2020). Consequently, the reported rates should be considered as potential rates
188 under moderately enriched conditions rather than strictly *in situ* rates (Dodds and Jones, 1987).
189 Additionally, incubations were conducted over 24 h, which may allow for processes such as
190 ammonia regeneration, microbial turnover, and grazing to influence substrate availability and
191 isotopic dilution. Although HgCl₂-poisoned controls and parallel measurements were used to
192 account for abiotic and background signals, these incubations cannot fully resolve short-term
193 dynamics or transient coupling between regeneration and oxidation processes. These
194 methodological constraints are inherent to low-rate measurements in oligotrophic systems
195 (Ward, 1985) and should be considered when interpreting the results. Another potential
196 caveate arising from the 24 h incubation is the potential production of unlabelled nitrite

197 via phytoplankton nitrate reduction (e.g., Travis et al., 2024) thereby diluting the $^{15}\text{NO}_2^-$ pool
198 leading to an underestimation of both ammonia and nitrite oxidation rates. In the present study,
199 however, primary production and ambient nitrite concentrations were low, suggesting that this
200 effect was likely limited in magnitude.

201

202 **2.3 Photosynthesis and Dark Carbon Fixation (DCF)**

203 Photosynthesis and chemoautotrophic DCF rates were measured using $\text{NaH}^{14}\text{CO}_3$
204 incorporation method (Steemann-Nielsen, 1952) with minor modifications (Reich et al., 2024,
205 2026). Triplicate seawater samples were collected from Niskin bottles in 50 ml acid-washed
206 falcon tubes and spiked with a diluted ‘working solution’ of $\text{NaH}^{14}\text{CO}_3$ (Perkin Elmer, specific
207 activity 56 mCi mmol^{-1}) at a final radioisotope dilution of $1:10^4$ v:v. Tubes were incubated in
208 the same tanks and under the same conditions used for the ammonia and nitrite oxidation
209 measurements with one exception – the DCF bottles were first covered with aluminum foil to
210 prevent light penetration. The tubes were incubated for 24 h before being filtered onto GF/F
211 filters ($0.7 \mu\text{m}$ nominal pore size, 25 mm diameter) using low vacuum pressure ($<50 \text{ mmHg}$).
212 The filters were placed in glass scintillation vials and $50 \mu\text{l}$ of 37% hydrochloric acid was added
213 to remove the non-fixed ^{14}C -bicarbonate overnight. Scintillation cocktail (5 ml, ULTIMA-
214 GOLD) was then added to each vial and samples were counted using a TRI-CARB 4810 TR
215 (Packard) liquid scintillation counter. Additional T_0 blanks were prepared by spiking bottles
216 with $\text{NaH}^{14}\text{CO}_3$ and filtering immediately (without incubation). Blanks consistently yielded
217 negligible activity. Added activity was measured by withdrawing $50 \mu\text{l}$ from random spiked
218 bottles (immediately after dosing and before incubation) and adding it onto a new GF/F filter
219 with $50 \mu\text{l}$ of ethanolamine ($\text{pH} \approx 12$) followed by scintillation cocktail and counting
220 immediately.

221 Photosynthesis was calculated as the difference between the disintegration per minute
222 (DPM) measured in the samples incubated under ambient irradiance and the dark bottles. DCF
223 and photosynthesis rates were calculated based on the Bermuda Atlantic Time-series Study
224 (BATS) protocol using the following Equation 4:

$$225 \quad (4) \text{ Production} = \frac{(DPM - \text{blank})}{V} \times DIC \times \frac{AA \text{ vol}}{TDPM} \times f \times \frac{1}{t}$$

226 Where, DPM equals the disintegrations per minute, V = the filtered volume (50 ml), DIC is the
227 dissolved inorganic carbon in seawater ($\sim 25 \text{ mg C L}^{-1}$, similar to other oceanic sites, (Knap and
228 Michaels, 1993), AA vol = Added activity volume (50 μl), TDPM = Total ^{14}C disintegration

229 per minute, t = incubation time (24h), and f = factor correcting isotope fractionation during
230 uptake of ^{14}C (1.05).

231

232 **2.4 Chlorophyll.*a* analysis**

233 Seawater samples (250 ml) were filtered onto Whatman GF/F filters at low pressure
234 (<150 mbar), placed in glass vials and frozen in the dark at -20 °C. Chlorophyll.*a* was extracted
235 with 5 ml of cold acetone (90%) overnight and determined by the non-acidification method
236 (Welschmeyer, 1994) using a Turner Designs (Trilogy) fluorometer.

237

238 **2.5 Statistical analysis**

239 Pairwise relationships between environmental variables and process rates were
240 evaluated using Pearson correlation coefficients calculated across all individual observations,
241 including all sampled depths (0-100 m) and stations. No prior averaging by depth or profile
242 was applied. Because many variables co-vary with depth and season, these correlations should
243 be interpreted as measures of co-variation rather than independent or causal relationships. Full
244 Pearson correlation statistics (r , r^2 , p -values) are provided in Supplementary Tables S1 and S2.
245 Statistical analyses were performed using Python.

246

247 **3 Results and discussion**

248 **3.1 Physiochemical and biological characteristics of the GoA during summertime**

249 Sampling spanned from late spring (May) to the end of summer (September) within the
250 euphotic zone (0-100 m) of the GoA. Surface temperatures ranged from ~25 °C in May to ~28
251 °C at the end of summer (September) and declined to ~23.5 °C at 100 m during all sampling
252 events (Figure 1A). Photosynthetic active radiation (PAR) levels ranged from ~1200-1950
253 $\mu\text{mol quanta m}^{-2} \text{ s}^{-1}$ at the surface and decreased exponentially to ~10-20 $\mu\text{mol quanta m}^{-2} \text{ s}^{-1}$
254 at 100 m (Figure 1B), corresponding to 0.5-1.8% of the surface irradiation levels. The
255 corresponding diffuse attenuation coefficient (K_d) was ~0.03-0.04 m^{-1} , in agreement with
256 previous observations from the GoA (Dishon et al., 2012; Stambler, 2006) as well as in other
257 oligotrophic regimes (Stambler, 2012). Concentrations of NH_4^+ ranged from undetectable to
258 65 nmol L^{-1} (Figure 1C). The corresponding integrated NH_4^+ inventory (0-100 m) was lowest
259 in May (1.68 $\mu\text{mol m}^{-2}$) and highest in July (~4.57 $\mu\text{mol m}^{-2}$) (Table 1). NO_2^- levels were
260 generally low throughout the upper 100 m (from below detection to <20 nmol L^{-1}), except in
261 September when nitrite increased with depth reaching ~45 nmol L^{-1} below 40 m (Figure 1D).
262 Vertical NO_2^- profiles suggest active ammonia oxidation below the strongly lit surface waters,

263 especially during September, although we cannot rule out expulsion of NO_2^- by phytoplankton
264 under light limitation (Berube et al., 2023; Collos, 1998). The vertically integrated NO_2^-
265 inventories ranged from 0.79-3.39 $\mu\text{mol m}^{-2}$ (Table 1). Surface NO_3^- was also low ($<20 \text{ nmol}$
266 L^{-1}) and generally increased with depth, suggesting organic matter regeneration and
267 nitrification during summertime (Figure 1E), and/or that less NO_3^- is assimilated by
268 phytoplankton at deeper depths. The integrated NO_3^- inventory ranged from 2.65 $\mu\text{mol m}^{-2}$ in
269 May and September up to 10.36 $\mu\text{mol m}^{-2}$ in June (Table 1). Collectively, the summertime
270 inorganic N species concentrations in the upper 100 m were low, in agreement with previous
271 reports from the oligotrophic GoA (Mackey et al., 2011; Meeder et al., 2012; Rahav et al.,
272 2015).

273 Chlorophyll *a* concentrations were low in the surface water ($<0.15 \mu\text{g L}^{-1}$) and
274 gradually increased with depth reaching maximal values in May and June ($\sim 0.60 \mu\text{g L}^{-1}$)
275 (Figure 2A). The corresponding integrated chlorophyll *a* was 26-28 mg m^{-2} except in August
276 where it was 16 mg m^{-2} (Table 1). As expected, photosynthesis rates were highest in the surface
277 water and decreased with depth (Figure 2B), coinciding with the decreasing PAR levels (Figure
278 1B). Photosynthesis rates decreased from $\sim 10 \mu\text{g C L}^{-1} \text{ d}^{-1}$ at the surface to below detection at
279 100 m, except in September when elevated rates were observed throughout the water column,
280 ranging from ~ 10 to 25 $\mu\text{g C L}^{-1} \text{ d}^{-1}$ (Figure 2B). The resulting integrated photosynthesis rates
281 ranged from 242 $\text{mg C m}^{-2} \text{ d}^{-1}$ in August to as high as 1263 $\text{mg C m}^{-2} \text{ d}^{-1}$ in September (Table
282 1). Despite the fluctuation in photosynthetic rates between months, these values are within the
283 range previously reported from the GoA (Rahav et al., 2015; Reich et al., 2024; Suggett et al.,
284 2009).

285 Chemoautotrophic DCF was lower than photosynthesis rates and exhibited no clear
286 vertical trends (Figure 2C). The surface DCF ranged from ~ 0.2 - $0.6 \mu\text{g C L}^{-1} \text{ d}^{-1}$ to ~ 0.1 - $0.9 \mu\text{g}$
287 $\text{C L}^{-1} \text{ d}^{-1}$ at 100 m (Figure 2C). The resulting integrated DCF ranged from 17-37 $\text{mg C m}^{-2} \text{ d}^{-1}$,
288 in agreement with a recent study from the GoA (Reich et al., 2024), corresponding to ~ 3 - 10%
289 of all the total autotrophic activity (photosynthesis and DCF combined). While multiple
290 microbial metabolisms involve chemoautotrophic carbon fixation, DCF is primarily attributed
291 to ammonia and nitrite oxidation, as these chemoautotrophic metabolisms are ubiquitous
292 throughout the oxic water column (Middelburg, 2011; Tang et al., 2023). In general, ammonia
293 oxidation likely provides energy that supports chemoautotrophic CO_2 assimilation throughout
294 the euphotic zone. Though less energy efficient, nitrite oxidation also contributes to DCF and
295 is considered especially relevant near the base of the euphotic zone where NO_2^- often
296 accumulates and reaches a maximum in concentration (Tang et al., 2023).

297

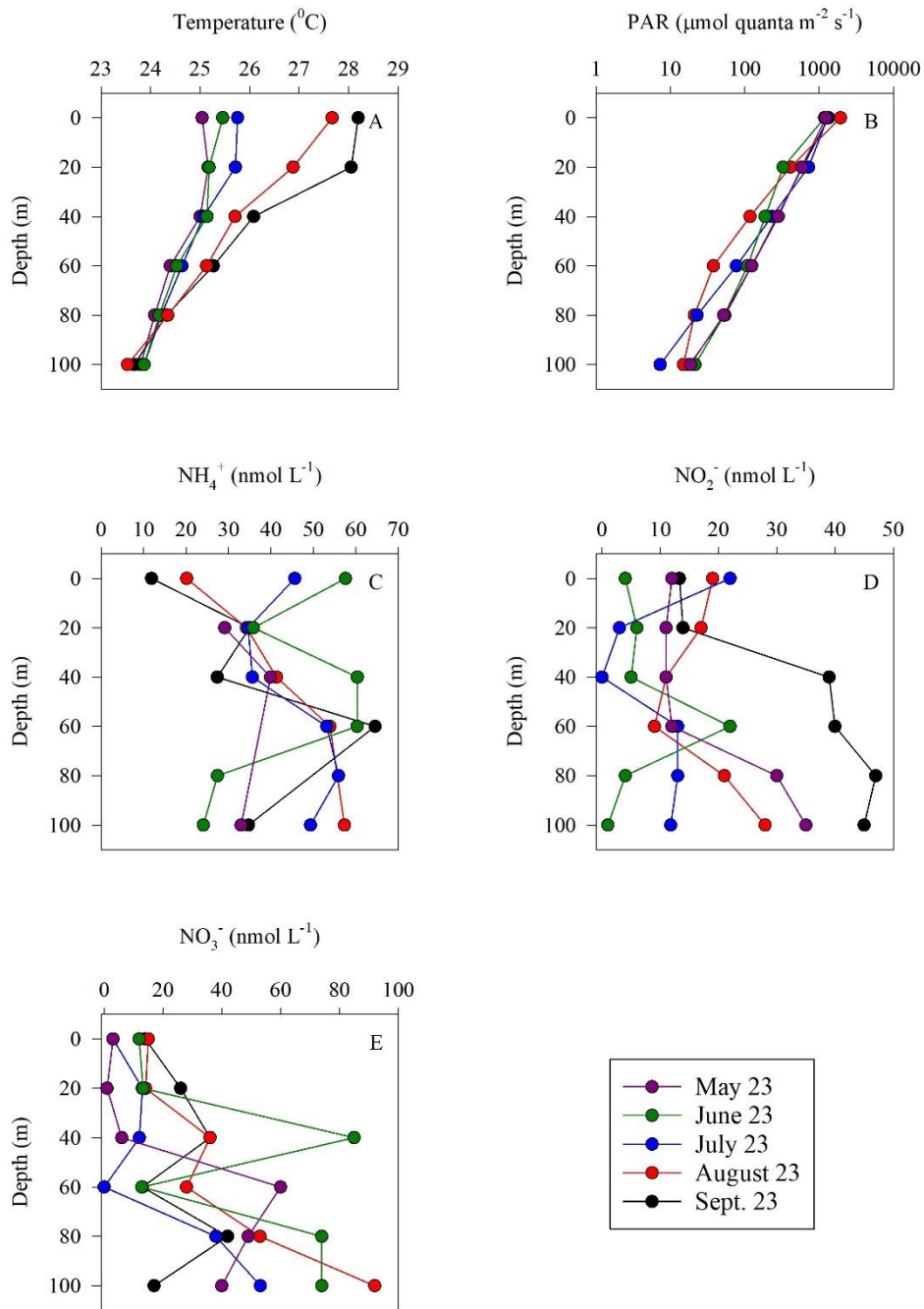
298 **Table 1:** Summary of integrated values (0-100 m) measured in the GoA (N Red Sea) during
 299 summer 2023.

Variable	May 23	June 23	July 23	Aug. 23	Sept. 23
Mixed layer depth (m)*	45	31	21	15	28
NH ₄ ⁺ (μmol m ⁻²)	1.68	4.54	4.57	3.36	2.99
NO ₂ ⁻ (μmol m ⁻²)	1.76	0.79	0.94	1.64	3.39
NO ₃ ⁻ (μmol m ⁻²)	2.76	10.36	6.60	6.13	2.65
Chlorophyll. <i>a</i> (mg m ⁻²)	26	28	26	16	28
Photosynthesis (mg C m ⁻² d ⁻¹)	350	349	302	242	1263
DCF (mg C m ⁻² d ⁻¹)	32	17	35	27	37
NH ₄ ⁺ oxidation (μmol m ⁻² d ⁻¹)	28	48	39	45	56
NO ₂ ⁻ oxidation (μmol m ⁻² d ⁻¹)	24	38	45	39	44
Contribution of NH ₄ ⁺ oxidation to DCF (%)**	0.32	1.02	0.40	0.60	0.54
Contribution of NO ₂ ⁻ oxidation to DCF (%)***	0.05	0.13	0.08	0.09	0.07

300 * Calculated from a temperature threshold criterion ($\Delta T = 0.2$ °C from surface values (de
 301 Boyer Montégut et al., 2004).

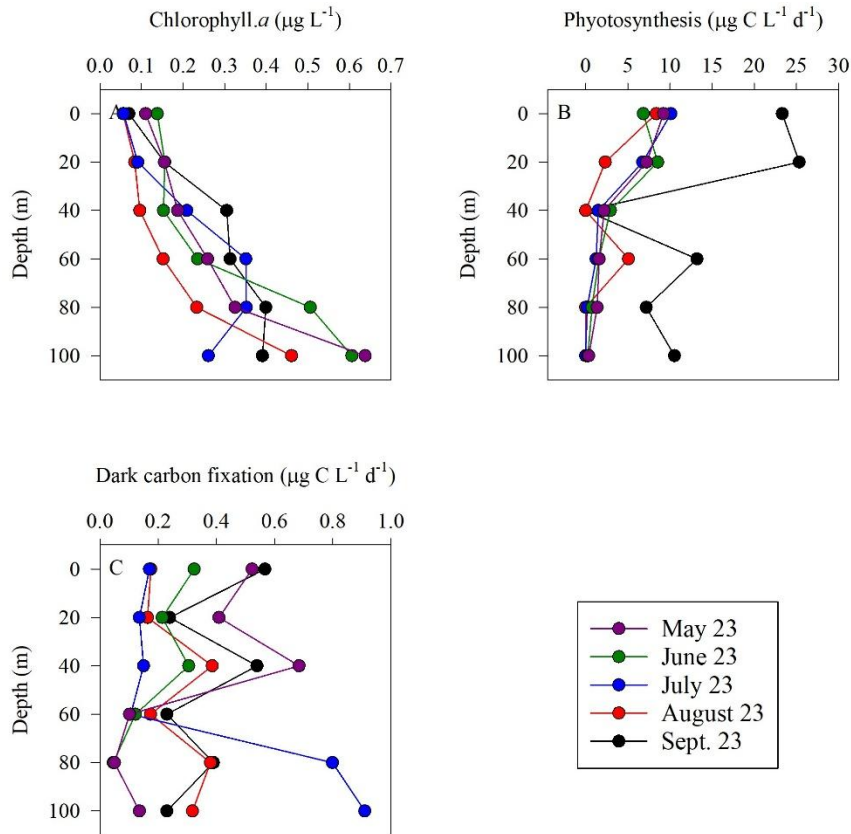
302 **Assuming 0.3 moles of C fixed per mole of NH₄⁺ oxidized (Santoro et al., 2010).

303 ***Assuming 0.05 moles of C per mole of NO₂⁻ oxidized (Beman et al., 2013).



304

305 **Figure 1:** Vertical distribution of temperature (A), PAR (B), NH_4^+ (C), NO_2^- (D) and NO_3^- (E)
 306 in the upper euphotic zone in the GoA, N Red Sea between May and September 2023.



307

308 **Figure 2:** Vertical distribution of chlorophyll-a (A), photosynthesis (B), and dark carbon
 309 fixation (C) in the upper euphotic zone in the GoA, N Red Sea between May and September
 310 2023.

311

312 3.2 Ammonia and nitrite oxidation rates

313 Ammonia and nitrite oxidation rates were generally low throughout the euphotic zone
 314 yet exhibited an increasing trend with depth (Figure 3), consistent with regulation by light
 315 inhibition. Overall, ammonia oxidation was homogeneous in the upper 40 m, ranging from
 316 ~ 0.10 - $0.55 \text{ nmol N L}^{-1} \text{d}^{-1}$. Below this depth rates increased towards the bottom of the euphotic
 317 zone ($\sim 100 \text{ m}$), ranging from ~ 0.26 - $0.83 \text{ nmol N L}^{-1} \text{d}^{-1}$ (Figure 3A,B). Ammonia oxidation
 318 rates often reached a maximum near the base of the euphotic zone (below the 50-100 m layer)
 319 as seen in other studies (reviewed by Tang et al., 2023). In general, these low euphotic zone
 320 ammonia oxidation rates are consistent with light inhibition, given the high PAR of the GoA
 321 during summer (Figure 1B, Wan et al., 2021). Competition of nitrifiers with phytoplankton for
 322 NH_4^+ may also result in low ammonia oxidation rates, as has been reported in the surface sunlit
 323 North Pacific (Smith et al., 2014). However, the highest integrated ammonia oxidation rate
 324 (September, $56 \mu\text{mol m}^{-2} \text{d}^{-1}$) was measured when chlorophyll.a levels and primary
 325 productivity were also relatively high and similar to springtime when the lowest ammonia

326 oxidation rates were measured (May, $28 \mu\text{mol m}^{-2} \text{d}^{-1}$) (Table 1). Thus, competition between
327 nitrifiers and phytoplankton for NH_4^+ does not appear to play a direct role in the regulation of
328 oxidation rates in our study. That said, the lack of correlation between chlorophyll *a* and
329 ammonia ($R^2=0.003$) does not preclude competition, but instead likely reflects rapid recycling
330 and tight coupling between ammonium production and uptake. Ammonia oxidation rates have
331 also been shown to be influenced by trace metal availability, specifically iron and copper
332 (Martocello and Wankel, 2024; Shafiee et al., 2019, 2021). However, given the close proximity
333 to major deserts, iron is not considered a limiting factor for microbes in the surface water of
334 the GoA (Chen et al., 2008; Torfstein et al., 2017). The limiting factors for ammonia oxidizers
335 in the GoA should be further studied by simulating different nutrients and temperature
336 scenarios with or without amendments of an inhibitor of ammonia monooxygenase to better
337 examine controls on environmental rates (Bayer et al., 2025).

338 During the study period, the mixed layer depth shoaled from ~ 45 m in May to ~ 15 m
339 in August (Table 1), reflecting progressive seasonal stratification. The vertical pattern of
340 ammonia oxidation (Figure 3) suggests that rates remained low throughout the strongly
341 illuminated upper water column, while modest increases at 60–80 m likely reflected reduced
342 light inhibition and/or more favorable conditions for nitrifier activity below the mixed layer.
343 Thus, unlike systems where ammonia oxidation increases sharply below the deep chlorophyll
344 maximum, nitrification in the GoA appears to follow a more gradual depth-related response
345 during stratified conditions.

346 As with ammonia oxidation, rates of nitrite oxidation also increased with depth (Figure
347 3C,D). Nitrite oxidation ranged from 0.14 to 0.70 $\text{nmol L}^{-1} \text{d}^{-1}$ (Figure 3C,D), with highest rates
348 measured over 80-100 m. Integrated nitrite oxidation rates were lowest in spring/early summer
349 ($\sim 24 \mu\text{mol m}^{-2} \text{d}^{-1}$) and increased between June to September ($38\text{-}45 \mu\text{mol m}^{-2} \text{d}^{-1}$) (Table 1).
350 Nitrite oxidation maxima (~ 100 m) were deeper than those of ammonia oxidation (~ 60 m).
351 This vertical offset may reflect differences in substrate supply and the decoupling of ammonia
352 and nitrite oxidation along the water column in addition to differential sensitivity to light (Wan
353 et al., 2021). ³For example, ammonium supply may be more closely linked to shallower
354 regeneration processes, whereas nitrite can accumulate and persist at greater depths (Travis et
355 al., 2024). At the same time, near-zero ambient NO_2^- or NO_3^- at specific depths and months
356 (e.g., 40 m for ammonia oxidation and 60 m for nitrite oxidation in July; Figure 1) should not
357 be interpreted as the absence of substrate availability, but as evidence of tight coupling between
358 substrate supply and demand over the incubation period. Nevertheless, isotopic measurements
359 at ambient concentrations of only a few tens of nmol L^{-1} carry greater analytical uncertainty

360 than measurements at higher concentrations, and the corresponding rate estimates are best
361 viewed as conservative lower bounds on nitrification activity.

362 Our results demonstrate that ammonia and nitrite oxidation ~~occurring~~ occurred at
363 comparable rates, which is consistent with the typically low concentrations of NO_2^- observed
364 in the GoA during summertime (Figure 1D, Meeder et al., 2012), and consistent with the low
365 net accumulation of NO_2^- resulting from limited decoupling between the two steps of
366 nitrification. Converting photosynthesis to nitrogen demand using Redfield stoichiometry (C:N
367 ≈ 6.6) suggests that phytoplankton nitrogen requirements in surface waters may substantially
368 exceed the measured nitrification rates. This implies that regenerated nitrogen, including
369 ammonium, is rapidly consumed, potentially limiting its availability for ammonia-oxidizing
370 microorganisms. However, this inference is based on carbon-derived estimates of
371 phytoplankton demand rather than direct measurements of nitrogen uptake and should therefore
372 be interpreted cautiously. Nevertheless, previous studies indicate that ammonia uptake can
373 greatly exceed nitrification rates in oligotrophic surface waters (Mackey et al., 2011).

374 To assess substrate control, we examined the relationship between NH_4^+ concentration
375 and ammonia oxidation rates across depths. This relationship was weak overall (Pearson,
376 $r \approx 0.30$), whereas rates were more strongly associated with depth ($r \approx 0.75$), indicating a
377 dominant role of depth-related gradients (Figure S1, Table S1). When examined by depth
378 intervals (0-50 m vs. 50-100 m), the NH_4^+ -oxidation relationship was weak in the upper 50 m
379 ($r \approx 0.23$) and stronger >50 m ($r \approx 0.41$) (Figure S1, Table S1). This suggests that rapid recycling
380 and competitive uptake weaken NH_4^+ -oxidation rate coupling in surface waters, whereas
381 reduced light inhibition at depth allows a somewhat greater influence of NH_4^+ . These results
382 are consistent with previous studies showing that nitrification maxima are often decoupled
383 from NH_4^+ peaks and instead reflect depth-dependent ecological structuring (Beman et al.,
384 2012).

385 Note that a key consideration in interpreting the measured rates is the relative magnitude of the
386 $^{15}\text{NH}_4^+$ tracer addition compared to ambient substrate concentrations. In the upper euphotic
387 zone, where NH_4^+ concentrations were often near detection limits (Figure 1), the addition of
388 $\sim 20 \text{ nmol L}^{-1}$ (tracer) represented a substantial enrichment of the available pool. Under such
389 conditions, if ammonia oxidation were strongly substrate-limited, one might expect a
390 measurable stimulation of rates. However, the observed rates remained consistently low across
391 depths and sampling periods (Table 1; Figure 3), even under these 'enriched' conditions. This
392 suggests that factors other than immediate substrate availability exert primary control over
393 ammonia oxidation in the upper waters of the GoA. These may include low abundances of

394 ammonia-oxidizing archaea (Aizawa et al., 2023; Smith et al., 2016), strong light inhibition in
395 surface waters (Figure 1B), or physiological constraints associated with oligotrophic adaptation
396 (Yin et al., 2024; Zhou et al., 2024). Rather than indicating the absence of substrate limitation
397 *per se*, our results imply that ammonia oxidation operates under a combination of ecological
398 and environmental constraints that limit its overall contribution to nitrogen cycling in this
399 system. Moreover, the use of 24 h incubations introduce additional uncertainty, as internal
400 recycling of ammonium and microbial interactions may partially decouple measured rates from
401 instantaneous *in situ* conditions. Therefore, the rates reported here are interpreted as
402 conservative estimates of nitrification potential in the upper euphotic zone. Adding to that, in
403 oligotrophic systems, rapid recycling of dissolved inorganic nitrogen can influence both
404 substrate availability (Christie-Oleza et al., 2017) and isotopic enrichment during incubation
405 experiments (Stukel, 2020). Thus, processes such as ammonium regeneration and microbial
406 uptake may dilute the ¹⁵N substrate pool or reduce accumulation of labelled products (Braun et
407 al., 2018). However, we surmise that any such processes, if occurred here, would tend to reduce
408 the apparent isotopic enrichment and thus bias rate estimates toward underestimation. Another
409 possible limitation regards the uncertainty in low nutrient concentrations in the GoA (most
410 notably within the upper mixed layer depth) that may propagate into rate calculations, as
411 substrate concentrations are explicitly included in the rate equations (see equations 1-3).
412 However, such uncertainty affects absolute rate estimates proportionally and does not alter the
413 overall interpretation of low nitrification activity. Accordingly, the reported rates should be
414 considered conservative estimates of nitrification activity over the incubation period. Future
415 work in similar ultra-oligotrophic settings could benefit from newer low-concentration nitrate
416 and nitrite isotope protocols (e.g., Jiang et al., 2026), which explicitly target sub nanomolar N
417 species.

418

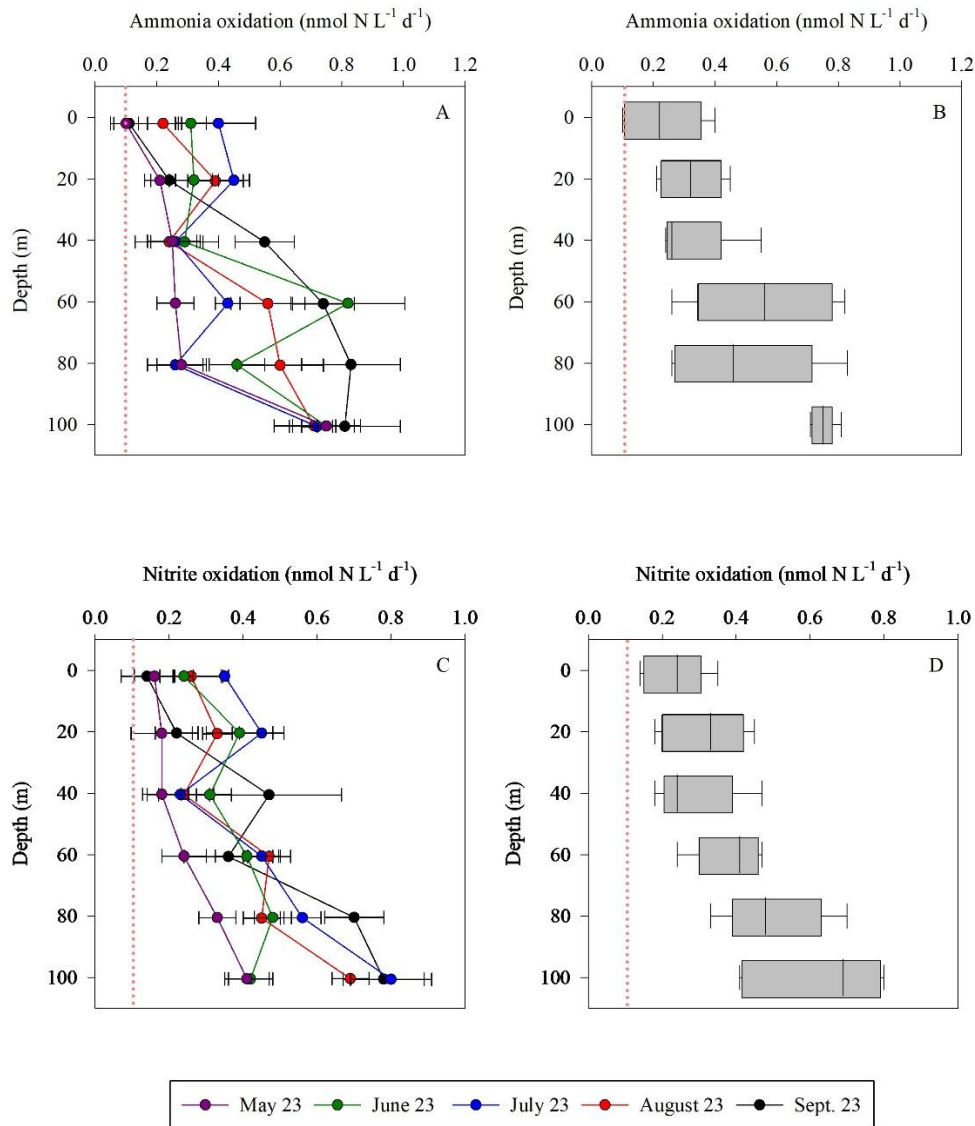
419 **3.3 Contribution of ammonia and nitrite oxidation to DCF**

420 DCF is widely thought to be dominated by ammonia and nitrite oxidation, as these
421 metabolic processes provide energy that, in turn, support chemoautotrophic CO₂ assimilation
422 (Middelburg, 2011), although additional pathways such as urea oxidation by ammonia
423 oxidizers may also contribute (Wan et al., 2024). While other chemoautotrophic metabolisms,
424 such as sulfur oxidation, anammox or methanotrophy also represent important drivers of
425 chemoautotrophy in some environments, these are unlikely to be relevant in the oxic,
426 oligotrophic waters of the GoA. DCF and nitrification are rarely measured simultaneously,
427 which prevents robust assessment of this relationship. Here, we explored DCF under the warm,

428 high-light, nutrient-poor conditions found in the GoA (Figure 1) and investigated how it relates
429 to corresponding rates of nitrification over the euphotic zone. We calculated the contribution
430 of ammonia and nitrite oxidation to DCF assuming 0.3 moles of C fixed per mole of NH_4^+
431 (Santoro et al., 2010). Overall, the depth-integrated contribution of ammonia oxidation to DCF
432 ranged between 0-2%, consistent, yet often lower than reports from other oceanographic
433 settings. For example, ammonia oxidizers contributed only a small fraction to DCF in the
434 eastern tropical Pacific, accounting for <20% of depth-integrated rates (Bayer et al., 2025). The
435 depth-integrated contribution of nitrite oxidation to DCF was negligible, accounting for 0.05-
436 0.13% (Table 1). Thus, ammonia and nitrite oxidation together could account for only ~1% of
437 the DCF, lower than recent estimates from the eastern tropical Pacific (Bayer et al., 2025),
438 though similar to observations in culture experiments with ammonia oxidizers (Bayer et al.,
439 2023). It is notable, however, that relevant conversion factors between moles C fixed per mole
440 of N oxidized in the ocean should be better constrained (and may be site-specific) (Tang et al.,
441 2023), which could alter the calculated contribution discussed here. Nevertheless, we show that
442 ammonia and nitrite oxidation link N recycling with inorganic carbon assimilation in the
443 euphotic zone in the GoA, and while their contribution to total primary production is relatively
444 small, it may sustain part of the microbial metabolism in the nutrient-depleted surface waters
445 of the GoA. Our results suggest that other microbial metabolism processes (e.g., anaplerosis)
446 may also contribute to DCF in the GoA's euphotic zone and should be estimated separately in
447 future studies.

448 DCF in the sunlit ocean should not be interpreted solely as nitrification-driven
449 chemoautotrophy. Even under dark incubation conditions, inorganic carbon fixation may
450 include contributions from phytoplankton-associated dark metabolism, heterotrophic inorganic
451 carbon assimilation, and other microbial pathways (Baltar and Herndl, 2019; Reich et al.,
452 2026). A recent 10-year analysis from the GoA (same study site) showed that DCF is a
453 persistent but variable component of carbon cycling, contributing substantially to total
454 autotrophic carbon fixation (Reich et al., 2024). Therefore, while our data suggests that
455 ammonia and nitrite oxidation contribute only a minor fraction of total DCF, the remaining
456 DCF signal likely reflects multiple unresolved microbial processes (Reich et al., 2025).

457



458

459 **Figure 3:** Vertical distribution of ammonia oxidation (A,B) and nitrite oxidation (C,D) in the
 460 upper euphotic zone in the GoA, N Red Sea between May and September 2023. The Box
 461 Whisker plots sum the data distribution per depth (n=5). The pink dashed line signifies the
 462 detection limit.

463

464 3.4 Environmental divers affecting ammonia and nitrite oxidation

465 Nitrification is known to be affected by PAR, oxygen levels, temperature, nitrogen
 466 substrate availability, pH, as well as by other environmental factors (Ward, 2008). Our results
 467 are consistent overall with previous observations at other sites as both ammonia and nitrite
 468 oxidation rates linearly correlate with most of these environmental variables, either positively
 469 or negatively (Figure 4; Figure S1; Tables S1 and S2). Most notably, ammonia and nitrite
 470 oxidation rates correlated with increasing depth and decreasing PAR level, consistent with
 471 previous reports showing that light inhibit nitrifier growth and nitrification rates (Merbt et al.,

472 2012; Olsen, 1989; Xu et al., 2019). Temperature correlated negatively with ammonia and
473 nitrite oxidation rates (Figure 4, $r=0.61$, $p<0.01$), likely reflects substrate limitation rather than
474 a direct temperature effect. Previous studies showed that increasing temperature generally
475 stimulates nitrification by simultaneously altering substrate availability and enzyme kinetics
476 (Emerson et al., 1975). As temperature increases, the pKa of the NH_4^+ - NH_3 system decreases,
477 shifting the equilibrium toward NH_3 , the putative substrate of ammonia monooxygenase
478 (Emerson et al., 1975). In parallel, warming enhances enzymatic activity, accelerating the
479 catalytic steps of both ammonia and nitrite oxidation (Zheng et al., 2017, 2020). We surmise
480 that in the stratified GoA, warming strengthened stratification, enhanced photo-inhibition, and
481 thereby increased biological competition for ammonium, thus reducing substrate supply to
482 nitrifiers despite favorable enzyme kinetics, leading to the observed negative correlation
483 between temperature and nitrification. In agreement with this line of thought, substrate
484 availability was positively correlated with ammonia oxidation (NH_4^+ , NO_2^-) and nitrite
485 oxidation (NO_2^- , NO_3^-), highlighting the substrate-dependent nature of nitrification.
486 Alternatively, these relationships may reflect co-variation with depth and associated
487 environmental gradients, rather than direct substrate control alone (discussed below). Ammonia
488 oxidation requires NH_4^+ or NH_3 as the electron donor, while nitrite oxidation depends on NO_2^-
489 availability. Elevated ambient concentrations of these substrates make them more available to
490 nitrifying enzymes, resulting in higher reaction rates until enzymatic saturation or co-limitation
491 with other nutrients are reached (e.g., vitamins and other co-factors, PO_4^{+}). In oligotrophic
492 systems such as the GoA, where ambient NH_4^+ and NO_2^- concentrations are exceptionally low,
493 even small pulses of reduced or intermediate nitrogen (e.g., from organic matter
494 remineralization, mixing, or atmospheric deposition) may trigger an increase in nitrification
495 rates.

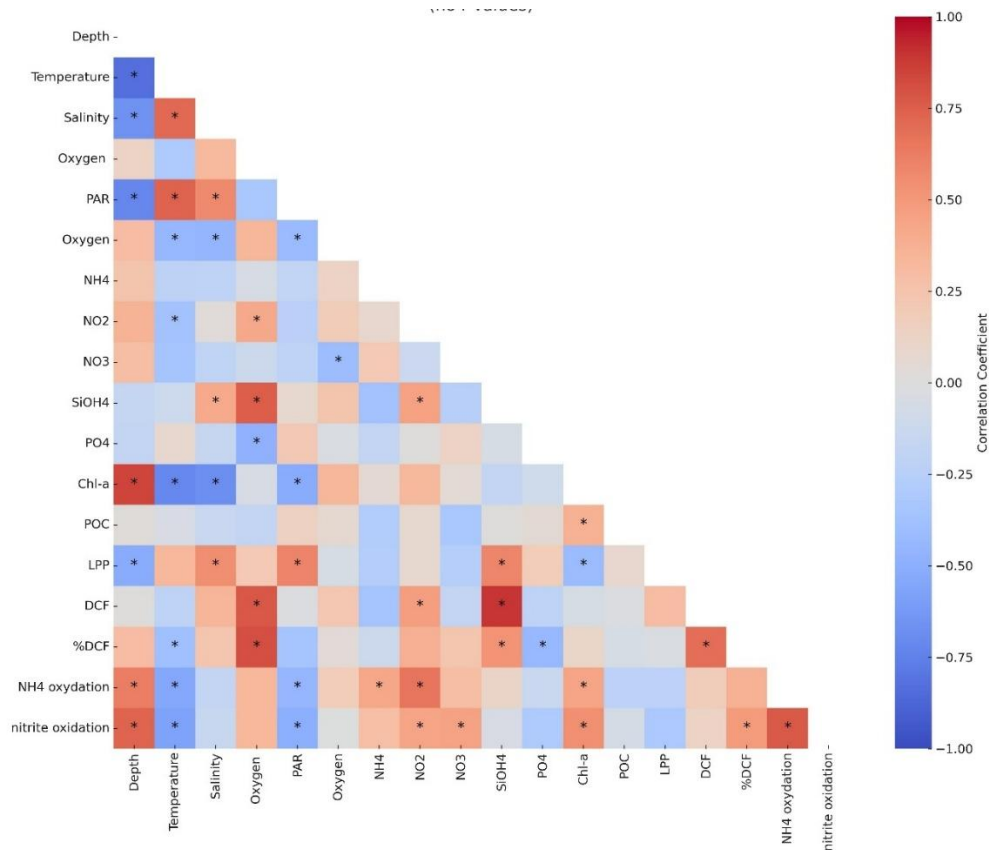
496 Nitrification is generally expected to show a negative relationship with chlorophyll.*a*
497 in surface waters, where phytoplankton may compete with nitrifiers for reduced nitrogen
498 species. Consequently, most studies report suppressed ammonia and nitrite oxidation rates near
499 the surface and enhanced rates below the chlorophyll maximum once light levels decrease and
500 substrate regeneration through organic matter remineralization becomes more important
501 (Beman et al., 2013; Yool et al., 2007). Here, however, we observed a positive correlation
502 between chlorophyll.*a* and ammonia or nitrite oxidation (as well as with photosynthesis,
503 although not significantly). This pattern likely reflects conditions near the deep chlorophyll
504 maximum (~80-100 m), where chlorophyll *a* is elevated due to photo-acclimation under low
505 light conditions rather than strictly higher biomass (Cornec et al., 2021; Fennel and Boss, 2003;

506 Scofield et al., 2020). In these depths, reduced irradiance and enhanced organic matter turnover
507 may promote ammonium regeneration, providing substrate that supports nitrification. These
508 findings suggest that the expected negative coupling at the surface is offset by strong
509 regeneration and oxidation processes near the deep chlorophyll maxima, resulting in an overall
510 positive relationship when integrated across the euphotic zone.

511 We expected that ammonia and nitrite oxidation would show a significant correlation
512 with DCF (see discussion above). Nevertheless, although both ammonia and nitrite oxidation
513 were positively coupled with DCF ($r=0.49$ and 0.17 , respectively), the correlations were not
514 statistically significant ($p>0.05$) and is in line with the overall low contribution of these
515 processes to DCF (discussion above and see Table 1). This suggests that additional pathways
516 such as anaplerotic processes may contribute to DCF (Dijkhuizen and Harder, 1984; Erb, 2011),
517 as well as other chemoautotrophic metabolisms beyond nitrification such as urea oxidation,
518 sulfur oxidation and iron oxidation (Arandia-Gorostidi et al., 2024; Dang and Chen, 2017),
519 while the contribution of ammonia and nitrite oxidation to total DCF is low (Table 1).

520 We note that correlation analysis should be interpreted with caution. Many parameters
521 considered here co-vary with depth (e.g., PAR, chlorophyll.*a*) and seasonal stratification
522 (mixed layer depth), which can produce strong apparent relationships without implying direct
523 mechanistic coupling. Furthermore, as the dataset is restricted to the upper 100 m, it does not
524 capture the full vertical structure of nitrification, including deeper maxima often observed
525 below the deep chlorophyll maximum. Accordingly, these correlations primarily reflect
526 processes operating within the upper euphotic zone and should not be extrapolated beyond this
527 depth range. Lastly, while variations in ammonia oxidation rates broadly co-occurred with
528 changes in primary production and chlorophyll *a*, these relationships should be interpreted with
529 caution. In this study, phytoplankton activity was assessed using carbon-based proxies, and no
530 direct measurements of nitrogen uptake or community composition were conducted. Therefore,
531 any inferred coupling between phytoplankton dynamics and nitrification remains indirect. The
532 observed patterns are consistent with the expectation that phytoplankton influence the
533 availability and cycling of regenerated nitrogen, but do not allow us to disentangle the relative
534 roles of substrate competition, regeneration, or microbial community structure. Future studies
535 that combine measurements of phytoplankton nitrogen demand, ammonium regeneration, and
536 nitrifier abundance and activity will be required to directly resolve these interactions in
537 oligotrophic systems.

538
539



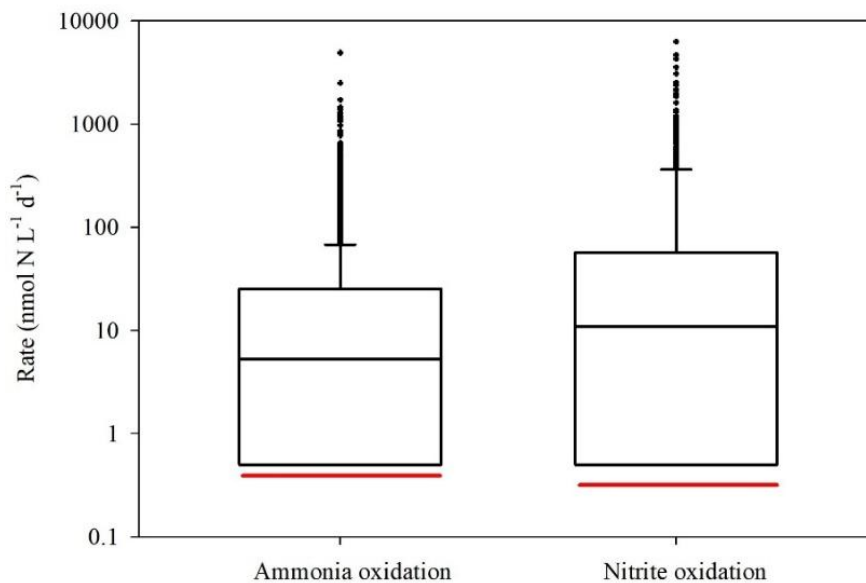
540

541 **Figure 4:** A heatmap showing Pearson correlation coefficients among measured environmental
 542 parameters and biogeochemical rates. Color shading indicates the strength and direction of the
 543 correlation. Asterisks denote statistically significant correlations ($p < 0.05$). Full descriptive
 544 statistics for the correlations are provided in the Supplementary Tables S1 and S2.

545

546 4 Conclusions

547 Globally, ammonia and nitrite oxidation rates in the euphotic zone span several orders
 548 of magnitude across offshore oceanic environments (Tang et al., 2023, Figure 5). The rates we
 549 measured in the GoA during summer fall below the global median (i.e., the red vs. black lines
 550 in Figure 5). The reason for the low rates in GoA is attributed to the low substrate availability
 551 during summertime (Figure 1C-E) but likely reflect a combination of environmental and
 552 ecological constraints rather than a single controlling factor. For example, the combination of
 553 high light intensity (Figure 1B) and penetration (i.e., $K_d \approx 0.04 \text{ m}^{-1}$) and enhanced stratification
 554 (Figure 1A) can further suppress nitrifier activity, either through photoinhibition of ammonia
 555 monooxygenase and/or by pushing microbial communities closer to their thermal tolerance
 556 limits. Moreover, the absence of measurements of nitrifier abundance preclude us from
 557 distinguishing whether low bulk rates reflect low population size or potentially high per-cell
 558 activity.



559

560 **Figure 5:** A literature compilation of reported euphotic zone's ammonia oxidation and nitrite
 561 oxidation recently reviewed Tang et al., (2023) and this study. The black line inside the boxes
 562 shows the median value of all studies considered, while the red line indicates the median values
 563 measured in the GoA during this study. Data include only offshore euphotic-zone
 564 measurements as defined in the original studies. We note that the depth and definition of the
 565 euphotic zone vary among regions, which may contribute to variability in reported rates.

566

567 Additionally, while our results suggest a potential linkage between phytoplankton
 568 activity and nitrogen cycling, this inference is based on carbon-derived proxies (primary
 569 production and chlorophyll.*a*) rather than direct measurements of species-specific nitrogen
 570 uptake or microbial community composition using genetic markers. Resolving this coupling
 571 will require future studies that simultaneously quantify phytoplankton nitrogen demand,
 572 ammonium regeneration, and nitrifier abundance and activity.

573 Future studies should focus on resolving the temporal and spatial variability of
 574 nitrification rates and nitrifier communities in the context of ongoing climate change. This is
 575 especially true for the GoA that experience rapid warming and ocean acidification. Long-term
 576 time series and diel-scale observations are needed to capture seasonal, interannual, and daily
 577 dynamics, particularly in relation to stratification, warming, and nutrient supply. Advanced
 578 molecular approaches such as metagenomics, metatranscriptomics, and single-cell tools should
 579 be applied to link community composition and functional potential with *in-situ* rate
 580 measurements. Parallel measurements of trace metals will be essential to assess their role as
 581 cofactors or inhibitors of key enzymes in ammonia and nitrite oxidation. Furthermore, the
 582 contribution of nitrification to DCF appears to be limited, suggesting that additional microbial

583 pathways contribute to inorganic carbon fixation in this system. Constraining these
584 contributions will require future studies that integrate rate measurements with microbial
585 community and metabolic analyses to better resolve the sources of DCF in oligotrophic waters.
586 Ultimately, combining high-resolution field observations with targeted manipulations and
587 modelling will improve our ability to predict how nitrification responds to environmental
588 change and contributes to current and future ocean nitrogen cycling.

589 *Data availability.* All the data is presented in the graphs/table/text and will be made available
590 in excel format upon request.

591 *Author contributions.* Conceptualized and conducted the field measurements; ER. Data
592 curation, formal analysis, and visualization; ER, SDW and AP. The paper was prepared by ER,
593 SDW and AP.

594 *Competing interests.* The contact author has declared that none of the authors has any
595 competing interests.

596 *Acknowledgments.* The authors thank the personnel in the Inter University Institute for Marine
597 Sciences in Eilat (IUI). This paper was supported by a grant from the Middle East Regional
598 Cooperation (MERC) (M39-011) to ER and AP. We also thank the two anonymous reviewers
599 for their constructive comments, which helped to significantly improve and refine the
600 manuscript.

601 **References**

- 602 Aizawa, A., Watanabe, Y., Hashioka, K., Kadoya, A., Suzuki, S., Yoshimura, T., and Kudo,
603 I.: Contribution of ammonium oxidizing archaea and bacteria to intensive nitrification during
604 summer in Mutsu Bay, Japan, *Reg. Stud. Mar. Sci.*, 63, 102984,
605 <https://doi.org/https://doi.org/10.1016/j.rsma.2023.102984>, 2023.
- 606 Arandia-Gorostidi, N., Jaffe, A. L., Parada, A. E., Kapili, B. J., Casciotti, K. L., Salcedo, R.
607 S. R., Baumas, C. M. J., and Dekas, A. E.: Urea assimilation and oxidation support activity of
608 phylogenetically diverse microbial communities of the dark ocean, *ISME J.*, 18,
609 <https://doi.org/10.1093/ismejo/wrae230>, 2024.
- 610 Baltar, F. and Herndl, G.: Is dark carbon fixation relevant for oceanic primary production
611 estimates?, *Biogeosciences Discuss.*, 1–12, <https://doi.org/10.5194/bg-2019-223>, 2019.
- 612 Bayer, B., McBeain, K., Carlson, C. A., and Santoro, A. E.: Carbon content, carbon fixation
613 yield and dissolved organic carbon release from diverse marine nitrifiers, *Limnol. Oceanogr.*,
614 68, 84–96, <https://doi.org/https://doi.org/10.1002/lno.12252>, 2023.
- 615 Bayer, B., Kitzinger, K., Paul, N. L., Albers, J. B., Saito, M. A., Wagner, M., Carlson, C. A.,
616 and Santoro, A. E.: Minor contribution of ammonia oxidizers to inorganic carbon fixation in

617 the ocean, *Nat. Geosci.*, 18, 1144–1151, <https://doi.org/10.1038/s41561-025-01798-x>, 2025.

618 Beman, J. M., Chow, C.-E., King, A. L., Feng, Y., Fuhrman, J. A., Andersson, A., Bates, N.
619 R., Popp, B. N., and Hutchins, D. A.: Global declines in oceanic nitrification rates as a
620 consequence of ocean acidification, *Proc. Natl. Acad. Sci.*, 108, 208–213,
621 <https://doi.org/10.1073/pnas.1011053108>, 2011.

622 Beman, J. M., Leilei Shih, J., and Popp, B. N.: Nitrite oxidation in the upper water column
623 and oxygen minimum zone of the eastern tropical North Pacific Ocean, *ISME J.*, 7, 2192–
624 2205, <https://doi.org/10.1038/ismej.2013.96>, 2013.

625 Berube, P. M., J., O. T., Anna, R., Trent, L., and W., C. S.: Production and cross-feeding of
626 nitrite within *Prochlorococcus* populations, *MBio*, 14, e01236-23,
627 <https://doi.org/10.1128/mbio.01236-23>, 2023.

628 de Boyer Montégut, C., Madec, G., Fischer, A. S., Lazar, A., and Iudicone, D.: Mixed layer
629 depth over the global ocean: An examination of profile data and a profile-based climatology,
630 *J. Geophys. Res. Ocean.*, 109, C12003, <https://doi.org/https://doi.org/10.1029/2004JC002378>,
631 2004.

632 Braun, J., Mooshammer, M., Wanek, W., Prommer, J., Walker, T. W. N., Rütting, T., and
633 Richter, A.: Full ¹⁵N tracer accounting to revisit major assumptions of ¹⁵N isotope pool
634 dilution approaches for gross nitrogen mineralization, *Soil Biol. Biochem.*, 117, 16–26,
635 <https://doi.org/https://doi.org/10.1016/j.soilbio.2017.11.005>, 2018.

636 Bristow, L. A., Sarode, N., Cartee, J., Caro-Quintero, A., Thamdrup, B., and Stewart, F. J.:
637 Biogeochemical and metagenomic analysis of nitrite accumulation in the Gulf of Mexico
638 hypoxic zone, *Limnol. Oceanogr.*, 60, 1733–1750,
639 <https://doi.org/https://doi.org/10.1002/lno.10130>, 2015.

640 Buchwald, C., Homola, K., Spivack, A. J., Estes, E. R., Murray, R. W., and Wankel, S. D.:
641 Isotopic constraints on nitrogen transformation rates in the deep sedimentary marine
642 biosphere, *Global Biogeochem. Cycles*, 32, 1688–1702,
643 <https://doi.org/https://doi.org/10.1029/2018GB005948>, 2018.

644 Casciotti, K. L., Sigman, D. M., Hastings, M. G., Böhlke, J. K., and Hilkert, A.:
645 Measurement of the oxygen isotopic composition of nitrate in seawater and freshwater using
646 the denitrifier method., *Anal. Chem.*, 74, 4905–4912, <https://doi.org/10.1021/ac020113w>,
647 2002.

648 Chen, Y., Paytan, A., Chase, Z., Measures, C., Beck, A. J., Sañudo-Wilhelmy, S. A., and
649 Post, A. F.: Sources and fluxes of atmospheric trace elements to the Gulf of Aqaba, Red Sea,
650 *J. Geophys. Res. Atmos.*, 113, 1–13, <https://doi.org/10.1029/2007JD009110>, 2008.

651 Christie-Oleza, J. A., Sousoni, D., Lloyd, M., Armengaud, J., and Scanlan, D. J.: Nutrient
652 recycling facilitates long-term stability of marine microbial phototroph-heterotroph
653 interactions, *Nat. Microbiol.*, 2, 17100, <https://doi.org/10.1038/nmicrobiol.2017.100>, 2017.

654 Clark, D. R., Rees, A. P., and Joint, I.: Ammonium regeneration and nitrification rates in the
655 oligotrophic Atlantic Ocean: Implications for new production estimates, *Limnol. Oceanogr.*,
656 53, 52–62, <https://doi.org/https://doi.org/10.4319/lo.2008.53.1.0052>, 2008.

657 Clark, D. R., Rees, A. P., Ferrera, C. M., Al-moosawi, L., Somerfield, P. J., Harris, C.,
658 Quartly, G. D., Goult, S., Tarran, G., and Lessin, G.: Nitrite regeneration in the oligotrophic
659 Atlantic Ocean, *Biogeosciences*, 19, 1355–1376, <https://doi.org/https://doi.org/10.5194/bg->

660 19-1355-2022, 2022.

661 Collos, Y.: Nitrate uptake, nitrite release and uptake, and new production estimates, *Mar.*
662 *Ecol. Prog. Ser.*, 171, 293–301, 1998.

663 Cornec, M., Claustre, H., Mignot, A., Guidi, L., Lacour, L., Poteau, A., D’Ortenzio, F.,
664 Gentili, B., and Schmechtig, C.: Deep chlorophyll maxima in the global ocean: occurrences,
665 drivers and characteristics, *Glob. Biochem. cycles*, 35, e2020GB006759,
666 <https://doi.org/10.1029/2020GB006759>, 2021.

667 Daims, H., Lebedeva, E. V., Pjevac, P., Han, P., Herbold, C., Albertsen, M., Jehmlich, N.,
668 Palatinszky, M., Vierheilig, J., Bulaev, A., Kirkegaard, R. H., von Bergen, M., Rattei, T.,
669 Bendinger, B., Nielsen, P. H., and Wagner, M.: Complete nitrification by *Nitrospira* bacteria,
670 *Nature*, 528, 504–509, <https://doi.org/10.1038/nature16461>, 2015.

671 Dang, H. and Chen, C.-T. A.: Ecological energetic perspectives on responses of nitrogen-
672 transforming chemolithoautotrophic microbiota to changes in the marine environment, *Front.*
673 *Microbiol.*, 8, 1246, <https://doi.org/10.3389/fmicb.2017.01246>, 2017.

674 Dijkhuizen, L. and Harder, W.: Current views on the regulation of autotrophic carbon dioxide
675 fixation via the Calvin cycle in bacteria, *Antonie Van Leeuwenhoek*, 50, 473–487, 1984.

676 Dishon, G., Dubinsky, Z., Caras, T., Rahav, E., Bar-Zeev, E., Tzuber, Y., and Iluz, D.:
677 Optical habitats of ultraphytoplankton groups in the Gulf of Eilat (Aqaba), Northern Red Sea,
678 *Int. J. Remote Sens.*, 33, 2683–2705, <https://doi.org/10.1080/01431161.2011.619209>, 2012.

679 Dodds, W. K. and Jones, R. D.: Potential rates of nitrification and denitrification in an
680 oligotrophic freshwater sediment system, *Microb. Ecol.*, 14, 91–100, 1987.

681 Emerson, K., Russo, R. C., Lund, R. E., and Thurston, R. V: Aqueous ammonia equilibrium
682 calculations: effect of pH and temperature, *J. Fish. Res. Board Canada*, 32, 2379–2383,
683 <https://doi.org/10.1139/f75-274>, 1975.

684 Eppley, R. W. and Peterson, B. J.: Particulate organic matter flux and planktonic new
685 production in the deep ocean, *Nature*, 282, 677–680, <https://doi.org/10.1038/282677a0>, 1979.

686 Erb, T. J.: Carboxylases in natural and synthetic microbial pathways,
687 <https://doi.org/10.1128/AEM.05702-11>, December 2011.

688 Fawcett, S. E., Lomas, M. W., Casey, J. R., Ward, B. B., and Sigman, D. M.: Assimilation of
689 upwelled nitrate by small eukaryotes in the Sargasso Sea, *Nat. Geosci.*, 4, 717–722,
690 <https://doi.org/10.1038/ngeo1265>, 2011.

691 Fei, X., Jian-Gong, W., Ting, Z., Bin, Z., Sung-Keun, R., and Zhe-Xue, Q.: Ubiquity and
692 diversity of complete ammonia oxidizers (Comammox), *Appl. Environ. Microbiol.*, 84,
693 e01390-18, <https://doi.org/10.1128/AEM.01390-18>, 2018.

694 Fennel, K. and Boss, E.: Subsurface maxima of phytoplankton and chlorophyll: Steady-state
695 solutions from a simple model, *Limnol. Oceanogr.*, 48, 1521–1534,
696 <https://doi.org/https://doi.org/10.4319/lo.2003.48.4.1521>, 2003.

697 Francis, C. A., Roberts, K. J., Beman, J. M., Santoro, A. E., and Oakley, B. B.: Ubiquity and
698 diversity of ammonia-oxidizing archaea in water columns and sediments of the ocean, *Proc.*
699 *Natl. Acad. Sci.*, 102, 14683–14688, <https://doi.org/10.1073/pnas.0506625102>, 2005.

700 Fuller, N. J., West, N. J., Marie, D., Yallop, M., Rivlin, T., Post, A. F., Interuniversity, T.,

701 Sciences, M., Beach, C., and Scanlan, D. J.: Dynamics of community structure and phosphate
702 status of picocyanobacterial populations in the Gulf of Aqaba , Red Sea, 50, 363–375, 2005.

703 Granger, J. and Sigman, D. M.: Removal of nitrite with sulfamic acid for nitrate N and O
704 isotope analysis with the denitrifier method, *Rapid Commun. Mass Spectrom.*, 23, 3753–
705 3762, <https://doi.org/10.1002/rcm.4307>, 2009.

706 Grasshoff, K., Kremling, K., and Ehrhardt, M.: *Methods of seawater analysis*, 3rd ed., edited
707 by: Kremling, K., Ehrenreich, I. M., and Grasshoff, K., Wiley, New York, 632 pp., 1999.

708 Henriksen, K. and Kemp, W. M.: Nitrification in estuarine and coastal marine sediments, in:
709 *Nitrogen Cycling in Coastal Marine Environments*, edited by: Blackburn, T. . and Sorensen,
710 J., John Wiley & Sons, Ltd, 207–249, 1988.

711 Herbert, R. A.: Nitrogen cycling in coastal marine ecosystems, *FEMS Microbiol. Rev.*, 23,
712 563–590, <https://doi.org/10.1111/j.1574-6976.1999.tb00414.x>, 1999.

713 Holms, R. ., Aminot, A., K erouel, R., Hooker, B. ., and Peterson, B. .: A simple and precise
714 method for measuring ammonium in marine and freshwater ecosystems, *Can. Data Rep. Fish.*
715 *Aquat. Sci.*, 56, 1801–1808, <https://doi.org/10.1139/cjfas-56-10-1801>, 1999.

716 Jiang, M., Koba, K., Ono, M., and Hayashi, K.: Improved isotopic analysis of low-
717 concentration freshwater nitrite by anion-exchange resin enrichment and azide reduction,
718 *Anal. Chem.*, 98, 2956–2967, <https://doi.org/10.1021/acs.analchem.5c05937>, 2026.

719 van Kessel, M. A. H. J., Speth, D. R., Albertsen, M., Nielsen, P. H., Op den Camp, H. J. M.,
720 Kartal, B., Jetten, M. S. M., and L ucker, S.: Complete nitrification by a single
721 microorganism, *Nature*, 528, 555–559, <https://doi.org/10.1038/nature16459>, 2015.

722 Mackey, K. R. M., Labiosa, R. G., Calhoun, M., Street, J. H., Post, A. F., and Paytan, A.:
723 Phosphorus availability, phytoplankton community dynamics, and taxon-specific phosphorus
724 status in the Gulf of Aqaba, Red Sea, *Limnol. Oceanogr.*, 52, 873–885,
725 <https://doi.org/10.4319/lo.2007.52.2.0873>, 2007.

726 Mackey, K. R. M., Bristow, L., Parks, D. R., Altabet, M. A., Post, A. F., and Paytan, A.: The
727 influence of light on nitrogen cycling and the primary nitrite maximum in a seasonally
728 stratified sea, *Prog. Oceanogr.*, 91, 545–560,
729 <https://doi.org/https://doi.org/10.1016/j.pocean.2011.09.001>, 2011.

730 Martocello, D. E. and Wankel, S. D.: Physiological influence of Fe and Cu availability on
731 nitrogen isotope fractionation during ammonia oxidation, *Environ. Sci. Technol.*, 58, 421–
732 431, <https://doi.org/10.1021/acs.est.3c05964>, 2024.

733 McIlvin, M. R. and Casciotti, K. L.: Technical updates to the bacterial method for nitrate
734 isotopic analyses, *Anal. Chem.*, 83, 1850–1856, <https://doi.org/10.1021/ac1028984>, 2011.

735 Mduyana, M., Thomalla, S. J., Philibert, R., Ward, B. B., and Fawcett, S. E.: The seasonal
736 cycle of nitrogen uptake and nitrification in the Atlantic sector of the Southern Ocean, *Global*
737 *Biogeochem. Cycles*, 34, e2019GB006363,
738 <https://doi.org/https://doi.org/10.1029/2019GB006363>, 2020.

739 Meeder, E., MacKey, K. R. M., Paytan, A., Shaked, Y., Iluz, D., Stambler, N., Rivlin, T.,
740 Post, A. F., and Lazar, B.: Nitrite dynamics in the open ocean-clues from seasonal and
741 diurnal variations, *Mar. Ecol. Prog. Ser.*, 453, 11–26, <https://doi.org/10.3354/meps09525>,
742 2012.

- 743 Merbt, S. N., Stahl, D. A., Casamayor, E. O., Martí, E., Nicol, G. W., and Prosser, J. I.:
744 Differential photoinhibition of bacterial and archaeal ammonia oxidation, *FEMS Microbiol.*
745 *Letts.*, 327, 41–46, <https://doi.org/10.1111/j.1574-6968.2011.02457.x>, 2012.
- 746 Michael Beman, J., Popp, B. N., and Alford, S. E.: Quantification of ammonia oxidation rates
747 and ammonia-oxidizing archaea and bacteria at high resolution in the Gulf of California and
748 eastern tropical North Pacific Ocean, *Limnol. Oceanogr.*, 57, 711–726,
749 <https://doi.org/https://doi.org/10.4319/lo.2012.57.3.0711>, 2012.
- 750 Middelburg, J. J.: Chemoautotrophy in the ocean, *Geophys. Res. Letts.*, 38, 94–97,
751 <https://doi.org/10.1029/2011GL049725>, 2011.
- 752 Mincer, T. J., Church, M. J., Taylor, L. T., Preston, C., Karl, D. M., and DeLong, E. F.:
753 Quantitative distribution of presumptive archaeal and bacterial nitrifiers in Monterey Bay and
754 the North Pacific Subtropical Gyre, *Environ. Microbiol.*, 9, 1162–1175,
755 <https://doi.org/https://doi.org/10.1111/j.1462-2920.2007.01239.x>, 2007.
- 756 Olsen, R.: Differential photoinhibition of marine nitrifying bacteria: a possible mechanism
757 for the formation of the primary nitrite maximum, *J. Mar. Syst.*, 31, 227–238, 1989.
- 758 Pachiadaki, M. G., Sintes, E., Bergauer, K., Brown, J. M., Record, N. R., Swan, B. K.,
759 Mathyer, M. E., Hallam, S. J., Lopez-Garcia, P., Takaki, Y., Nunoura, T., Woyke, T., Herndl,
760 G. J., and Stepanauskas, R.: Major role of nitrite-oxidizing bacteria in dark ocean carbon
761 fixation, *Science (80-.)*, 358, 1046–1051, <https://doi.org/10.1126/science.aan8260>, 2017.
- 762 Rahav, E., Herut, B., Mulholland, M. R., Belkin, N., Elifantz, H., and Berman-Frank, I.:
763 Heterotrophic and autotrophic contribution to dinitrogen fixation in the Gulf of Aqaba, *Mar.*
764 *Ecol. Prog. Ser.*, 522, 67–77, <https://doi.org/10.3354/meps11143>, 2015.
- 765 Reich, T., Belkin, N., Sisma-Ventura, G., Berman-Frank, I., and Rahav, E.: Significant dark
766 inorganic carbon fixation in the euphotic zone of an oligotrophic sea, *Limnol. Oceanogr.*,
767 9999, 1–14, <https://doi.org/10.1002/lno.12560>, 2024.
- 768 Reich, T., Belkin, N., Sisma-Ventura, G., Hauzer, H., Rubin-Blum, M., Berman-Frank, I.,
769 and Rahav, E.: Contribution of dark inorganic carbon fixation to bacterial carbon demand in
770 the oligotrophic Southeastern Mediterranean Sea, *Ocean Sci.*, 21, 3055–3067,
771 <https://doi.org/10.5194/os-21-3055-2025>, 2025.
- 772 Reich, T., Belkin, N., Sisma-ventura, G., Hauzer, H., Berman-frank, I., and Rahav, E.: Does
773 oligotrophy favor chemoautotrophy over photoautotrophy ?, *Prog. Oceanogr.*, 241, 103633,
774 <https://doi.org/10.1016/j.pocean.2025.103633>, 2026.
- 775 Santoro, A. E., Casciotti, K. L., and Francis, C. A.: Activity, abundance and diversity of
776 nitrifying archaea and bacteria in the central California current, *Environ. Microbiol.*, 12,
777 1989–2006, <https://doi.org/https://doi.org/10.1111/j.1462-2920.2010.02205.x>, 2010.
- 778 Scofield, A. E., Watkins, J. M., Osantowski, E., and Rudstam, L. G.: Deep chlorophyll
779 maxima across a trophic state gradient: A case study in the Laurentian Great Lakes., *Limnol.*
780 *Oceanogr.*, 65, 2460–2484, <https://doi.org/10.1002/lno.11464>, 2020.
- 781 Shafiee, R. T., Snow, J. T., Zhang, Q., and Rickaby, R. E. M.: Iron requirements and uptake
782 strategies of the globally abundant marine ammonia-oxidising archaeon, *Nitrosopumilus*
783 *maritimus* SCM1, *ISME J.*, 13, 2295–2305, <https://doi.org/10.1038/s41396-019-0434-8>,
784 2019.
- 785 Shafiee, R. T., Diver, P. J., Snow, J. T., Zhang, Q., and Rickaby, R. E. M.: Marine ammonia-

786 oxidising archaea and bacteria occupy distinct iron and copper niches, *ISME Commun.*, 1, 1,
787 <https://doi.org/10.1038/s43705-021-00001-7>, 2021.

788 Shiozaki, T., Ijichi, M., Fujiwara, A., Makabe, A., Nishino, S., Yoshikawa, C., and Harada,
789 N.: Factors regulating nitrification in the Arctic Ocean: potential impact of sea ice reduction
790 and ocean acidification, *Global Biogeochem. Cycles*, 33, 1085–1099,
791 <https://doi.org/https://doi.org/10.1029/2018GB006068>, 2019.

792 Sigman, D. M., Casciotti, K. L., Andreani, M., Barford, C., Galanter, M., and Böhlke, J. K.:
793 A bacterial method for the nitrogen isotopic analysis of nitrate in seawater and freshwater,
794 *Anal. Chem.*, 73, 4145–4153, <https://doi.org/10.1021/ac010088e>, 2001.

795 Smith, J. M., Damashek, J., Chavez, F. P., and Francis, C. A.: Factors influencing
796 nitrification rates and the abundance and transcriptional activity of ammonia-oxidizing
797 microorganisms in the dark northeast Pacific Ocean, *Limnol. Oceanogr.*, 61, 596–609,
798 <https://doi.org/https://doi.org/10.1002/lno.10235>, 2016.

799 Stambler, N.: Light and picophytoplankton in the Gulf of Eilat (Aqaba), *J. Geophys. Res.*,
800 111, C11009, 2006.

801 Stambler, N.: Underwater light field of the Mediterranean Sea, in: *Life in the Mediterranean*
802 *Sea: A Look at Habitat Changes*, edited by: Stambler, N., Nova Science Publishers, 1–739,
803 2012.

804 Steemann-Nielsen, E.: The use of radioactive carbon (¹⁴C) for measuring organic production
805 in the sea, *J. des Cons. Int. Pour Explor. la Mer*, 18, 117–140, 1952.

806 Stukel, M. R.: Investigating equations for measuring dissolved inorganic nutrient uptake in
807 oligotrophic conditions, *Limnol. Oceanogr. Methods*, 18, 656–672, 2020.

808 Suggett, D. J., Stambler, N., Prášil, O., Kolber, Z., Quigg, A., Vázquez-Dominguez, E.,
809 Zohary, T., Berman, T., Iluz, D., Levitan, O., Lawson, T., Meeder, E., Lazar, B., Bar-Zeev,
810 E., Medova, H., and Berman-Frank, I.: Nitrogen and phosphorus limitation of oceanic
811 microbial growth during spring in the Gulf of Aqaba, *Aquat. Microb. Ecol.*, 56, 227–239,
812 2009.

813 Tang, W., Ward, B. B., Beman, M., Bristow, L., Clark, D., Fawcett, S., Frey, C., Fripiat, F.,
814 Herndl, G. J., Mduyana, M., Paulot, F., Peng, X., Santoro, A. E., Shiozaki, T., Sintes, E.,
815 Stock, C., Sun, X., Wan, X. S., Xu, M. N., and Zhang, Y.: Database of nitrification and
816 nitrifiers in the global ocean, *Earth Sci. Rev.*, 15, 5039–5077,
817 <https://doi.org/https://doi.org/10.5194/essd-15-5039-2023>, 2023.

818 Torfstein, A., Teutsch, N., Tirosh, O., Shaked, Y., Rivlin, T., Zipori, A., Stein, M., Lazar, B.,
819 and Erel, Y.: Chemical characterization of atmospheric dust from a weekly time series in the
820 north Red Sea between 2006 and 2010, *Geochim. Cosmochim. Acta*, 211, 373–393,
821 <https://doi.org/10.1016/j.gca.2017.06.007>, 2017.

822 Travis, N. M., Kelly, C. L., and Casciotti, K. L.: Testing the influence of light on nitrite
823 cycling in the eastern tropical North Pacific, *Biogeosciences*, 21, 1985–2004,
824 <https://doi.org/10.5194/bg-21-1985-2024>, 2024.

825 Wan, X. S., Sheng, H.-X., Dai, M., Church, M. J., Zou, W., Li, X., Hutchins, D. A., Ward, B.
826 B., and Kao, S.-J.: Phytoplankton-nitrifier interactions control the geographic distribution of
827 nitrite in the upper ocean, *Global Biogeochem. Cycles*, 35, e2021GB007072,
828 <https://doi.org/https://doi.org/10.1029/2021GB007072>, 2021.

829 Wan, X. S., Sheng, H.-X., Shen, H., Zou, W., Tang, J.-M., Qin, W., Dai, M., Kao, S.-J., and
830 Ward, B. B.: Significance of Urea in Sustaining Nitrite Production by Ammonia Oxidizers in
831 the Oligotrophic Ocean, *Global Biogeochem. Cycles*, 38, e2023GB007996,
832 <https://doi.org/https://doi.org/10.1029/2023GB007996>, 2024.

833 Wankel, S. D., Kendall, C., Pennington, J. T., Chavez, F. P., and Paytan, A.: Nitrification in
834 the euphotic zone as evidenced by nitrate dual isotopic composition: Observations from
835 Monterey Bay , California, *Glob. Biochem. cycles*, 21, 1–13,
836 <https://doi.org/10.1029/2006GB002723>, 2007.

837 Ward, B. B.: Light and substrate concentration relationships with marine ammonium
838 assimilation and oxidation rates, *Mar. Chem.*, 16, 301–316,
839 [https://doi.org/https://doi.org/10.1016/0304-4203\(85\)90052-0](https://doi.org/https://doi.org/10.1016/0304-4203(85)90052-0), 1985.

840 Ward, B. B.: Nitrogen transformations in the Southern California Bight, *Deep Sea Res. Part*
841 *A. Oceanogr. Res. Pap.*, 34, 785–805, [https://doi.org/https://doi.org/10.1016/0198-](https://doi.org/https://doi.org/10.1016/0198-0149(87)90037-9)
842 [0149\(87\)90037-9](https://doi.org/https://doi.org/10.1016/0198-0149(87)90037-9), 1987.

843 Ward, B. B.: Nitrification in Marine Systems, in: *Nitrogen in the Marine Environment*
844 *Environment*, edited by: Capon, D. G., Bronk, D. A., Mulholland, M. R., and Carpenter, E.
845 J., Elsevier, 199–262, <https://doi.org/10.1016/B978-0-12-372522-6.00005-0>, 2008.

846 Welschmeyer, N. A.: Fluorometric analysis of chlorophyll a in the presence of chlorophyll b
847 and pheopigments, *Limnol. Oceanogr.*, 39, 1985–1992, 1994.

848 Wuchter, C., Abbas, B., Coolen, M. J. L., Herfort, L., van Bleijswijk, J., Timmers, P., Strous,
849 M., Teira, E., Herndl, G. J., Middelburg, J. J., Schouten, S., and Sinninghe Damsté, J. S.:
850 Archaeal nitrification in the ocean, *Proc. Natl. Acad. Sci.*, 103, 12317–12322,
851 <https://doi.org/10.1073/pnas.0600756103>, 2006.

852 Xu, M. N., Li, X., Shi, D., Zhang, Y., Dai, M., Huang, T., Glibert, P. M., and Kao, S.-J.:
853 Coupled effect of substrate and light on assimilation and oxidation of regenerated nitrogen in
854 the euphotic ocean, *Limnol. Oceanogr.*, 64, 1270–1283,
855 <https://doi.org/https://doi.org/10.1002/lno.11114>, 2019.

856 Yin, Q., He, K., Collins, G., De Vrieze, J., and Wu, G.: Microbial strategies driving low
857 concentration substrate degradation for sustainable remediation solutions, *npj Clean Water*, 7,
858 52, <https://doi.org/10.1038/s41545-024-00348-z>, 2024.

859 Yool, A., Martin, A. P., Fernández, C., and Clark, D. R.: The significance of nitrification for
860 oceanic new production, *Nature*, 447, 999–1002, <https://doi.org/10.1038/nature05885>, 2007.

861 Zheng, Z.-Z., Wan, X., Xu, M. N., Hsiao, S. S.-Y., Zhang, Y., Zheng, L.-W., Wu, Y., Zou,
862 W., and Kao, S.-J.: Effects of temperature and particles on nitrification in a eutrophic coastal
863 bay in southern China, *J. Geophys. Res. Biogeosciences*, 122, 2325–2337,
864 <https://doi.org/https://doi.org/10.1002/2017JG003871>, 2017.

865 Zheng, Z.-Z., Zheng, L.-W., Xu, M. N., Tan, E., Hutchins, D. A., Deng, W., Zhang, Y., Shi,
866 D., Dai, M., and Kao, S.-J.: Substrate regulation leads to differential responses of microbial
867 ammonia-oxidizing communities to ocean warming, *Nat. Commun.*, 11, 3511,
868 <https://doi.org/10.1038/s41467-020-17366-3>, 2020.

869 Zhou, Y., Yan, A., Yang, J., He, W., Guo, S., Li, Y., Wu, J., Dai, Y., Pan, X., Cui, D.,
870 Pereira, O., Teng, W., Bi, R., Chen, S., Fan, L., Wang, P., Liao, Y., Qin, W., Sui, S.-F., Zhu,
871 Y., Zhang, C., and Liu, Z.: Ultrastructural insights into cellular organization, energy storage

872 and ribosomal dynamics of an ammonia-oxidizing archaeon from oligotrophic oceans, *Front.*
873 *Microbiol.*, 15, 1367658, <https://doi.org/10.3389/fmicb.2024.1367658>, 2024.

874 Zhu, W., Wang, C., Hill, J., He, Y., Tao, B., Mao, Z., and Wu, W.: A missing link in the
875 estuarine nitrogen cycle? Coupled nitrification-denitrification mediated by suspended
876 particulate matter, *Sci. Rep.*, 8, 2282, <https://doi.org/10.1038/s41598-018-20688-4>, 2018.

877